Srrm234, but not canonical SR and hnRNP proteins drive inclusion of *Dscam* exon 9 variable exons

PINAR USTAOGLU[1†], IRMGARD U. HAUSSMANN[1,2], HONGZHI LIAO[1‡], ANTONIO TORRES-MENDEZ[3], ROLAND ARNOLD[4], MANUEL IRIMIA[3,5,6] AND MATTHIAS SOLLER[1,7]

Figure legends for Supplementary Figures

Supplementary Figure S1. Transposon inserts in SR protein genes. The genomic locus is depicted for the genes where transposon insertion alleles were analysed. The gene span is shown on top as blue box and below transcribed parts are shown as boxes for exons and lines for introns. Transposon insertions are shown as green triangles. Note that transposon have a size of ~10 kb and disrupt gene expression.

Supplementary Figure S2. Expression of *Dscam* (A) and *Srrm234* (B) in the nervous system of *Drosophila* late stage embryos as determined by RNA in situ hybridization.

Supplementary Figure S3. Transposon inserts in hnRNP protein genes. Transposon inserts in SR protein genes. The genomic locus is depicted for the genes where transposon insertion alleles were analysed. The gene span is shown on top as blue box and below transcribed parts are shown as boxes for exons and lines for introns. Transposon insertions are shown as green triangles. Note that transposon have a size of ~10 kb and disrupt gene expression.

Supplementary Figure S4. Hrp36, Hrp38, Hrp48 and Hrp40 SELEX motif occurrence is shown for the *Dscam* variable cluster 9 with the line indicating maximal amount of significant hits ($p<0.05$) of the SELEX motif in a sliding window (12 for Hrp36, 12 for Hrp38, 8 for Hrp48 and 9 for Hrp40).

Hrp36, Hrp38, Hrp48 and Hrp40 CLIP binding data from Blanchette et al. (2009) is shown for the *Dscam* variable cluster 9 with top and bottom lines indicating the binding score per tiling oligo probe (±0.54 for Hrp 36 and Hrp38, and ±49 for Hrp48 and Hrp40) compared to averaged binding score for all tiling oligos as determined by TiMAT.

Changes in exon inclusion as $\log_2$ fold change in LOF and GOF conditions are shown at the bottom.

Supplementary Figure S5. Vista plot alignment of *Dscam* exons 7 to 11 of the *D. melanogaster* sequence compared to the *D. virilis* sequence. Exons are shown as boxes on top and indicated in pink on the alignment. Constant exons are shown in orange and variable exons in light blue. Dark blue exons are absent in *D. virilis*, and exons only present in *D. virilis* are shon on top.

Supplementary Figure S6. Alignment of the short introns between variable exons from the exon 9 cluster of *D. melanogaster* (A) and *D. virilis* (D), and analysis for sequences complementary to the conserved sequence from intron 9.33 termed docking site (B, Yang et al, 2011). Longer introns with postulated selector sequences are shown at the bottom of the alignment. Sequences with base-pairing capacity to the intron 9.33 sequence termed docking site are shown for *D. melanogaster* (C) and *D. virilis* (E). Note that sequences with base-pairing capacity to the intron 9.33 sequence termed docking site are absent from most introns.

Supplementary Figure S7. Comparison of long-range base pairing potential of the docking site compared to 100 randomly chosen *Dscam* intronic sequences of the same length. (A) The distribution density of normalised alignment scores (filtered to have at maximum two gaps) against reverse and reverse complement sequences of the same length (docking: alignment scores for the docking sequence, randomly selected: 100 other sequences, see Material and Methods). (B) The same data, but showing the amount of sequences that pass the gap filtering threshold in both sets. (C) Density distribution of computed optimal secondary structures for each sequence. Vertical lines indicate the result for the docking sequence against the reverse and reverse-complement concatenated intronic sequences.

Supplementary Figure S1

X16: P{GSV6}Hrb27C^{GS16784}

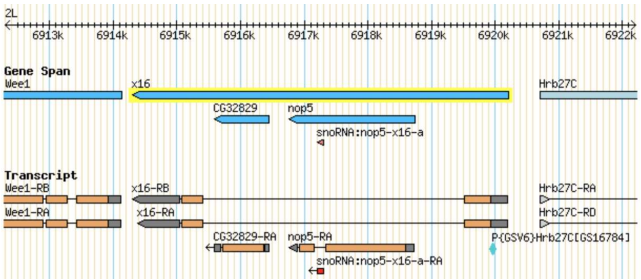

SF2: P{GSV7}SF2^{GS22325}

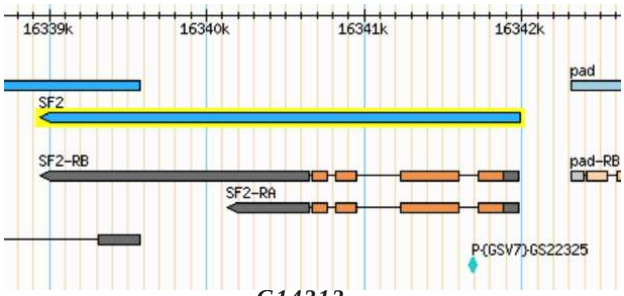

RBP1: P{EP}mRpL^{HP37044}

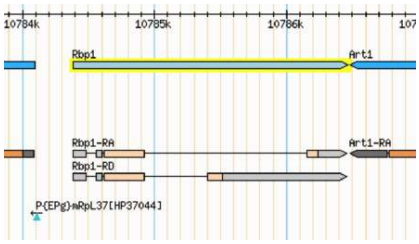

SF1: P{EP}SF1^{G14313}

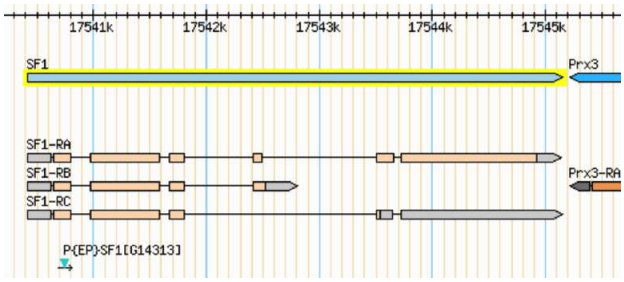

RBP1-like: P{GawB}RBP1-like^{NP0295}

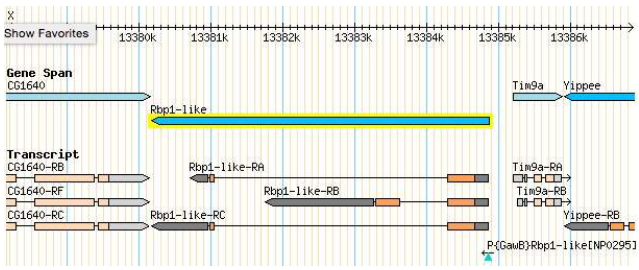

SRP54: P{GSV6}Srp54^{GS15334}

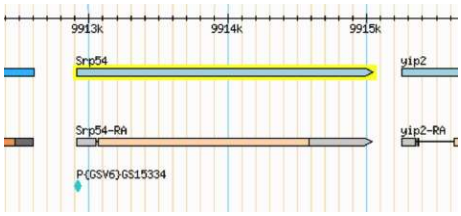

SC35: P{SUPor-P}SC35^{KG02986}

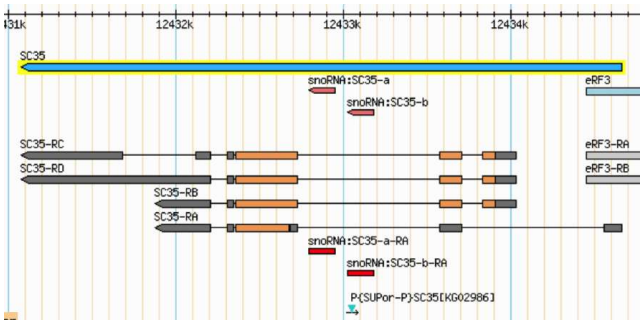

Supplementary Figure S2

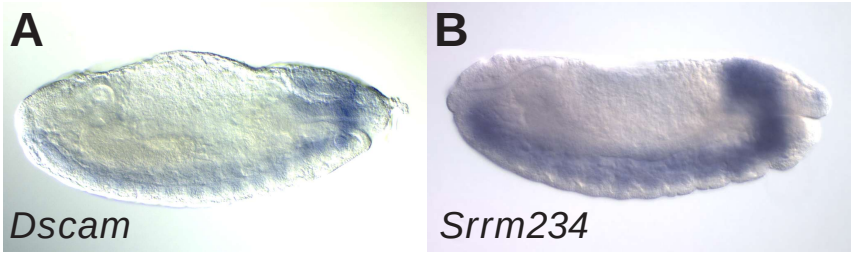

Supplementary Figure S3

Hrp38: Mi{MIC}Hrb98DE^{MI10594}

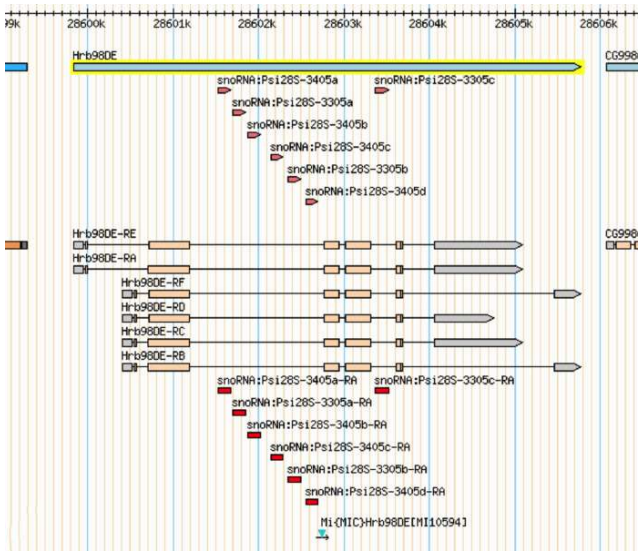

Hrp40: P{GSV6}sqd^{GS18188}

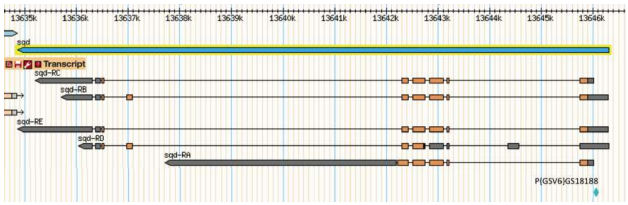

Glo: PBac{WH}glo^{f02674}

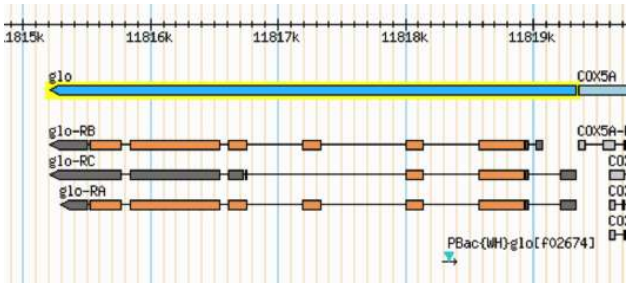

RB97d: P{PZ}Rb97D^{1}

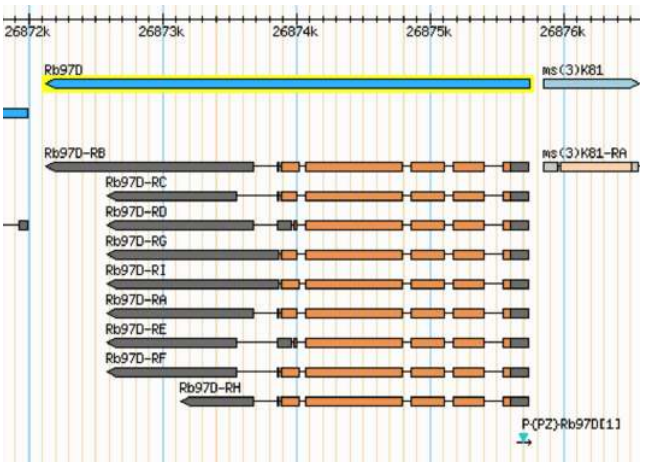

Hrb57A: P{EP}HnRNP-K^{G13574}

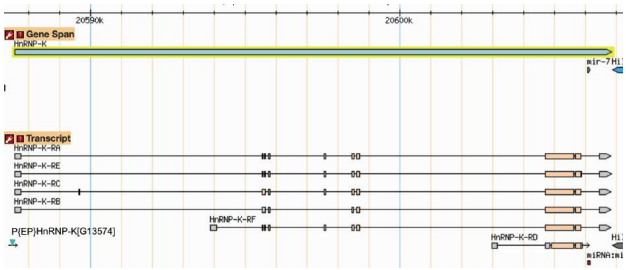

Hrp59: P{GSV3}rump^{GS6029}

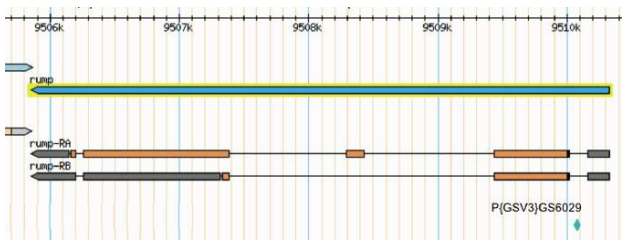

Hrp48: P{GSV6}Hrb27C^{GS14498}

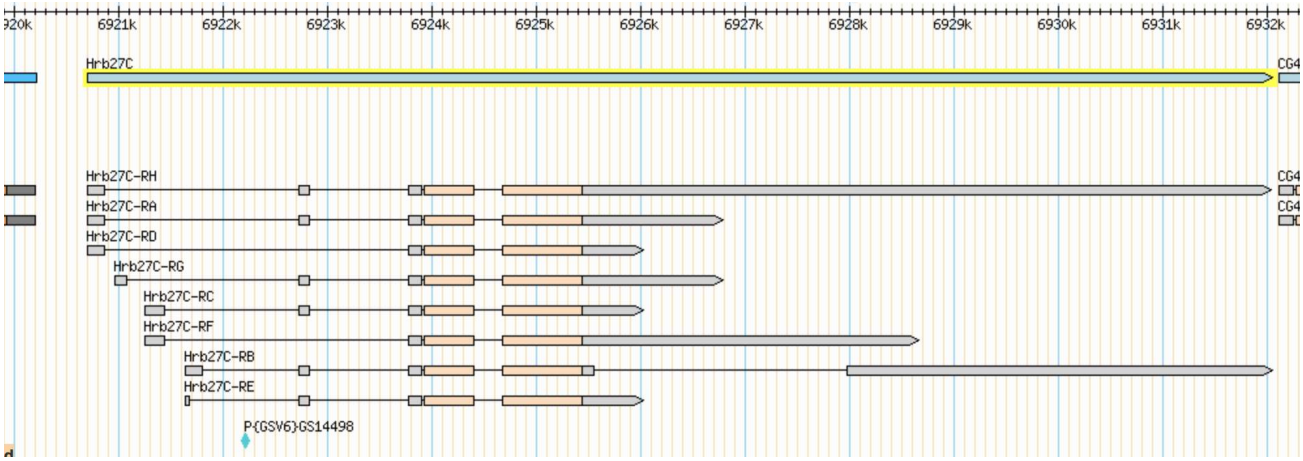

Supplementary Figure S4

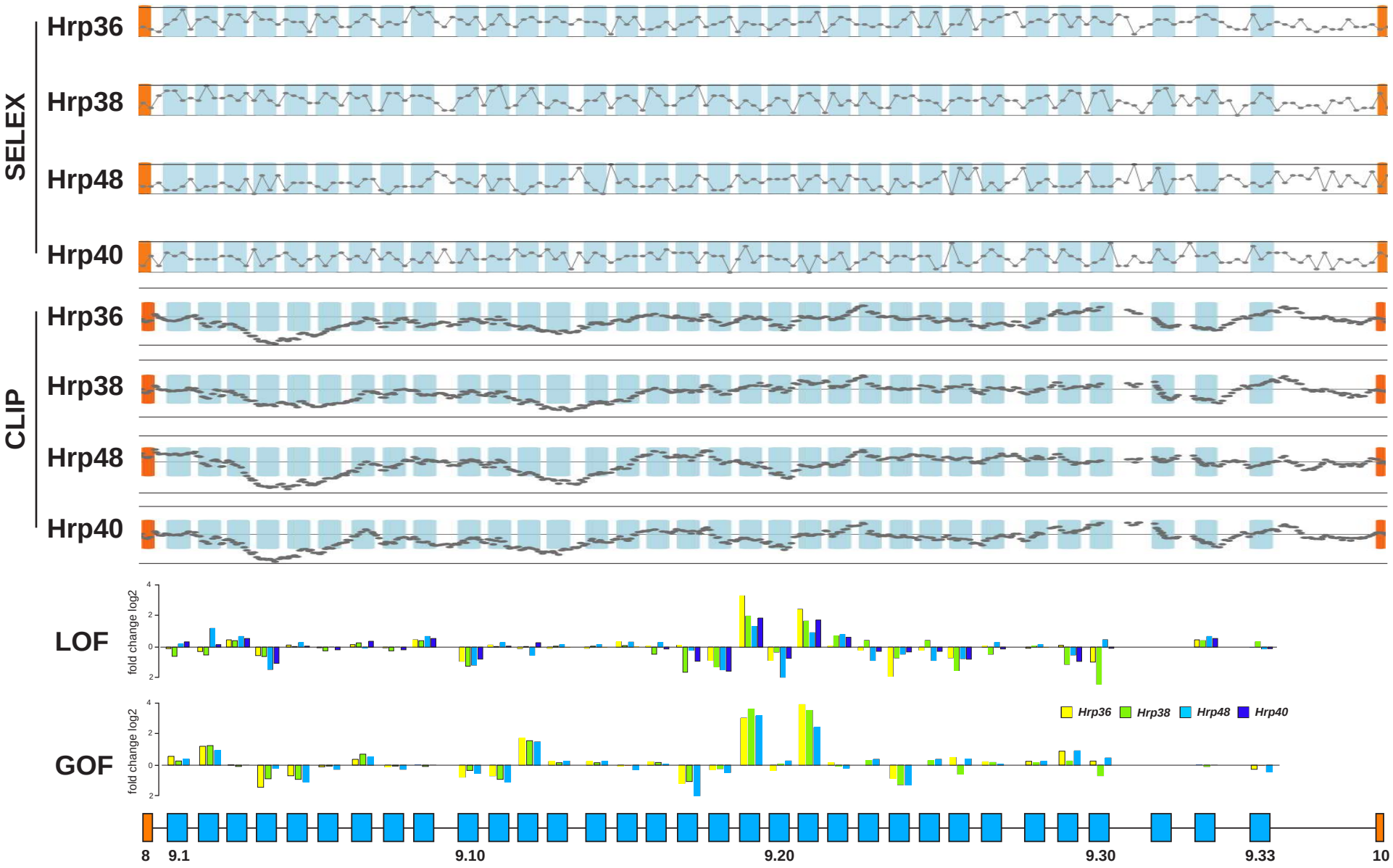

Supplementary Figure S5

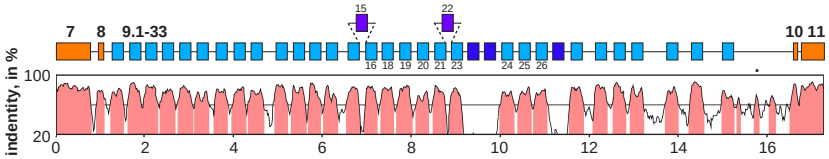

Supplementary Figure S6

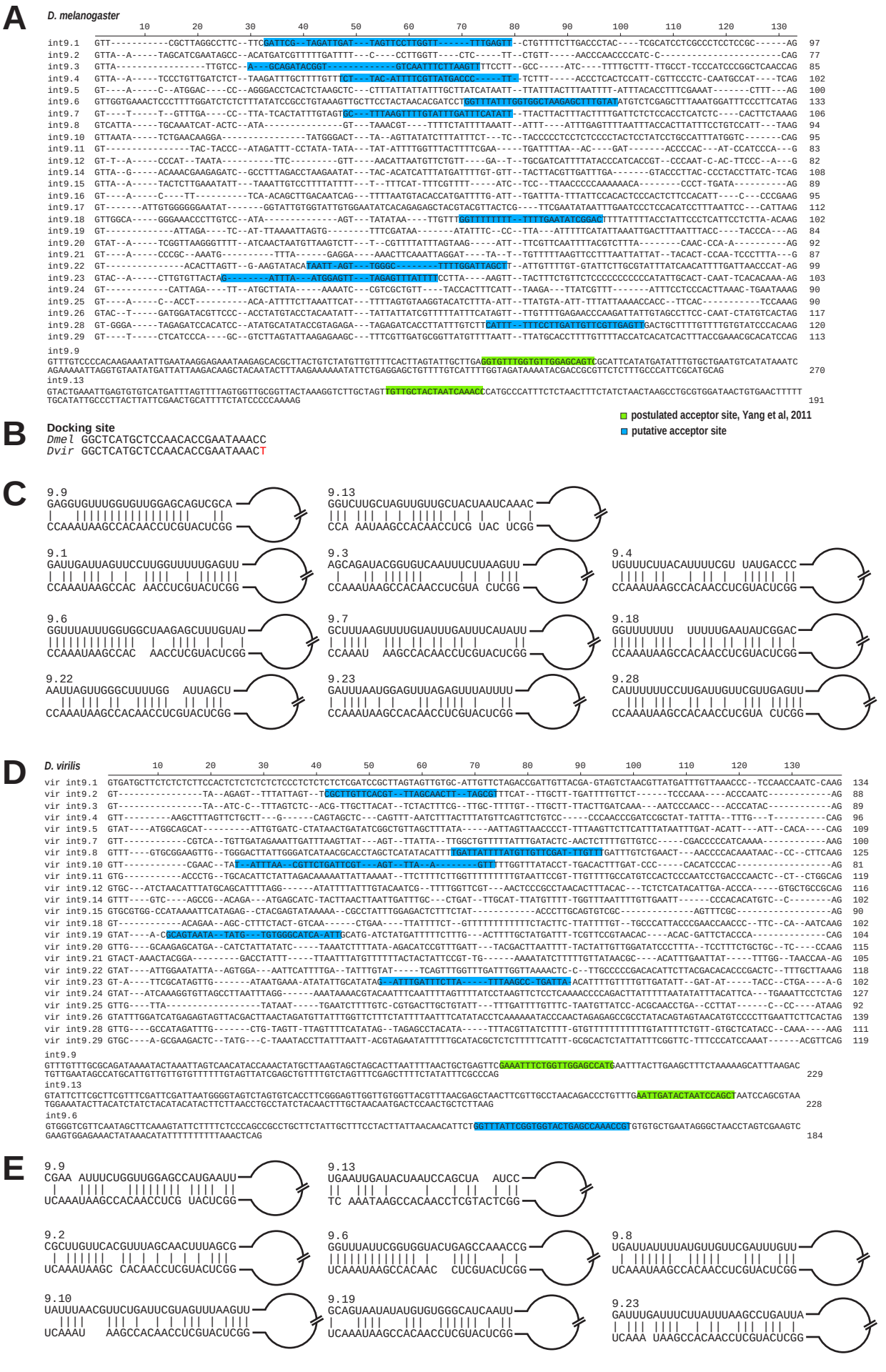

Supplementary Figure S7